A KRAB/KAP1-miRNA Cascade Regulates Erythropoiesis Through Stage-Specific Control of Mitophagy

Isabelle Barde,[1] Benjamin Rauwel,[1] Ray Marcel Marin-Florez,[2]* Andrea Corsinotti,[1]† Elisa Laurenti,[1]‡ Sonia Verp,[1] Sandra Offner,[1] Julien Marquis,[1]§ Adamandia Kapopoulou,[1] Jiri Vanicek,[2] Didier Trono[1]||

During hematopoiesis, lineage- and stage-specific transcription factors work in concert with chromatin modifiers to direct the differentiation of all blood cells. We explored the role of KRAB-containing zinc finger proteins (KRAB-ZFPs) and their cofactor KAP1 in this process. In mice, hematopoietic-restricted deletion of *Kap1* resulted in severe hypoproliferative anemia. *Kap1*-deleted erythroblasts failed to induce mitophagy-associated genes and retained mitochondria. This was due to persistent expression of microRNAs (miRNAs) targeting mitophagy transcripts, itself secondary to a lack of repression by stage-specific KRAB-ZFPs. The KRAB/KAP1-miRNA regulatory cascade is evolutionarily conserved, as it also controls mitophagy during human erythropoiesis. Thus, a multilayered transcription regulatory system is present, in which protein- and RNA-based repressors are superimposed in combinatorial fashion to govern the timely triggering of an important differentiation event.

Through the process of erythropoiesis, about 100 billion new red cells are generated every day in the human adult bone marrow. This process is initiated by the differentiation of hematopoietic stem cells (HSCs) into the earliest erythroid progenitor, which was identified ex vivo as a slowly growing burst-forming unit. This erythroid progenitor morphs into the rapidly dividing colony-forming unit, the proliferation of which is stimulated by the hypoxia-induced hormone erythropoietin. Further differentiation occurs through a highly sophisticated program orchestrated by lineage- and stage-specific combinations of protein- and RNA-based transcription regulators (*1*–*3*). It culminates in the elimination of intracellular organelles (including mitochondria and the nucleus) to yield the fully mature erythrocyte, containing on the order of 250 million molecules of hemoglobin as almost sole cargo. Much is still to be learned about the molecular mechanisms of these events, not only to understand the cause of red cell disorders, but also to aid the in vitro manufacturing of large supplies of oxygen-carrying cells for transfusion.

The genomes of higher vertebrates encode hundreds of KRAB-containing zinc finger proteins (KRAB-ZFPs) that can bind DNA in a sequence-specific fashion through a C-terminal array of C_2H_2 zinc fingers and can recruit the co-repressor KAP1 via their N-terminal KRAB domain (*4*–*7*). KAP1, also known as TRIM28 (tripartite motif protein 28), TIF1β (transcription intermediary factor 1β), or KRIP-1 (KRAB-interacting protein 1), acts as a scaffold for a multimolecular complex that silences transcription through the formation of heterochromatin (*8*–*11*). The KRAB/KAP1 system probably evolved initially to minimize retroelement-induced genome perturbations (*12*–*14*), but recent data indicate that it also regulates multiple aspects of mammalian physiology (*15*–*24*). The present study was undertaken to explore its role in hematopoiesis.

[1]School of Life Sciences and Frontiers in Genetics Program, Ecole Polytechnique Fédérale de Lausanne (EPFL), 1015 Lausanne, Switzerland. [2]School of Basic Sciences, EPFL, 1015 Lausanne, Switzerland.

*Present address: Center for Integrative Genomics, University of Lausanne, 1015 Lausanne, Switzerland.
†Present address: Centre for Genomic Regulation, 08003 Barcelona, Spain.
‡Present address: Campbell Family Institute for Cancer Research, Ontario Cancer Institute, Princess Margaret Cancer Centre, University Health Network and Department of Molecular Genetics, University of Toronto, Toronto, Ontario M5S 1A8, Canada.
§Present address: Functional Genomics Core, Nestlé Institute of Health Sciences, EPFL Campus, 1015 Lausanne, Switzerland.
||Corresponding author. E-mail: didier.trono@epfl.ch

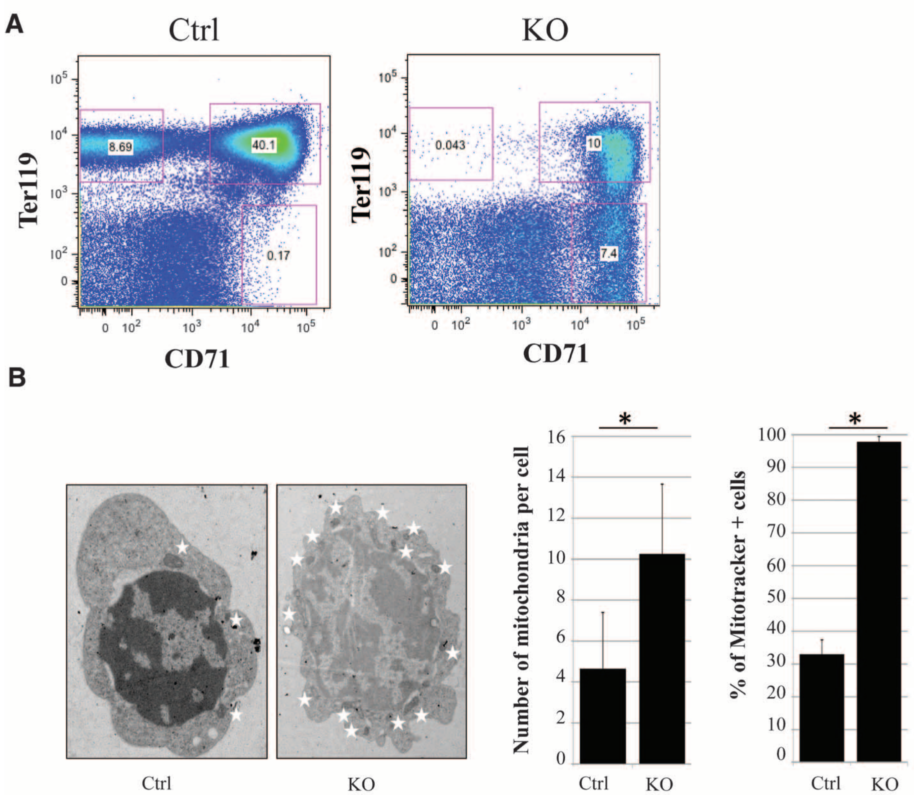

Fig. 1. Blocked erythrocyte maturation and accumulation of mitochondria in Kap1-deleted erythroblasts. (**A**) Fluorescence-activated cell sorting (FACS) analysis of CD71 and Ter119 in bone marrow from control (Ctrl) and *Kap1* KO mice 7 weeks after polyinosinic-polycytidylic acid injection. Percentage of each population from the total bone marrow is indicated. (**B**) Electron microscopy (left, stars indicate mitochondria; center, average number of mitochondria visualized per cell; $n = 10$, $*P < 0.05$) and MitoTracker staining (right, $n = 4$, $*P < 0.05$). Here and in other figures, error bars denote SD. Decreased nuclear density was frequent in *Kap1* KO cells, perhaps reflecting altered chromatin condensation.

The hemato-specific knockout of *Kap1* in the mouse, whereby the hematopoietic system of otherwise wild-type animals is reconstituted from *Kap1*-deleted hematopoietic stem cells and progenitors (fig. S1), resulted in a series of hematological abnormalities (table S1). Mutant mice displayed fatal hyporegenerative anemia, characterized by the accumulation of transferrin receptor/CD71^{+} glycophorin A–associated/Ter119^{-}

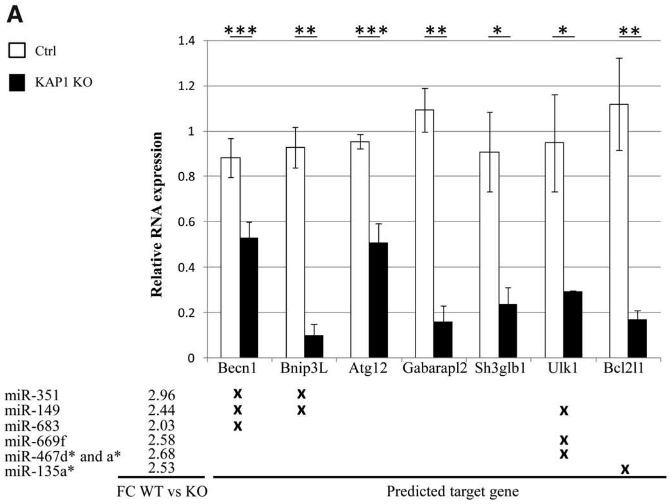

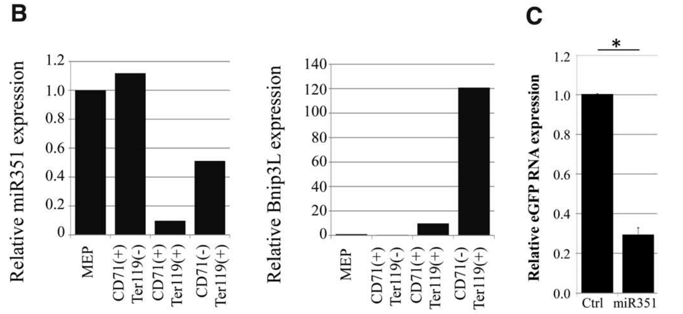

Fig. 2. A KAP1-miRNA cascade controls red cell mitophagy. (**A**) Top: Mitophagy-related transcripts in erythroblasts from control (Ctrl) and *Kap1* KO mice ($n = 4$, $*P < 0.05$, $**P < 0.01$, $***P < 0.001$). Bottom: Indicated miRNA expression in the same samples; X denotes predicted miRNA-target pairs. (**B**) miR-351 and Bnip3L expression in megakaryocyte/erythroid progenitors (MEP: Lin^{-} Sca1^{-} CD117^{+} CD34^{-} CD16.32^{-}, in which expression was set at 1) and indicated erythroblast subsets. (**C**) miR-351 targets the *Bnip3L* 3′UTR. Ctrl, for which the normalized value was set at 1, was a combination of MEL cells not overexpressing miR-351 and transduced with a GFP-expressing lentiviral vector with the *Bnip3L* 3′UTR, and cells overexpressing miR-351 but transduced with the same vector without this sequence ($n = 3$, $*P < 0.05$).

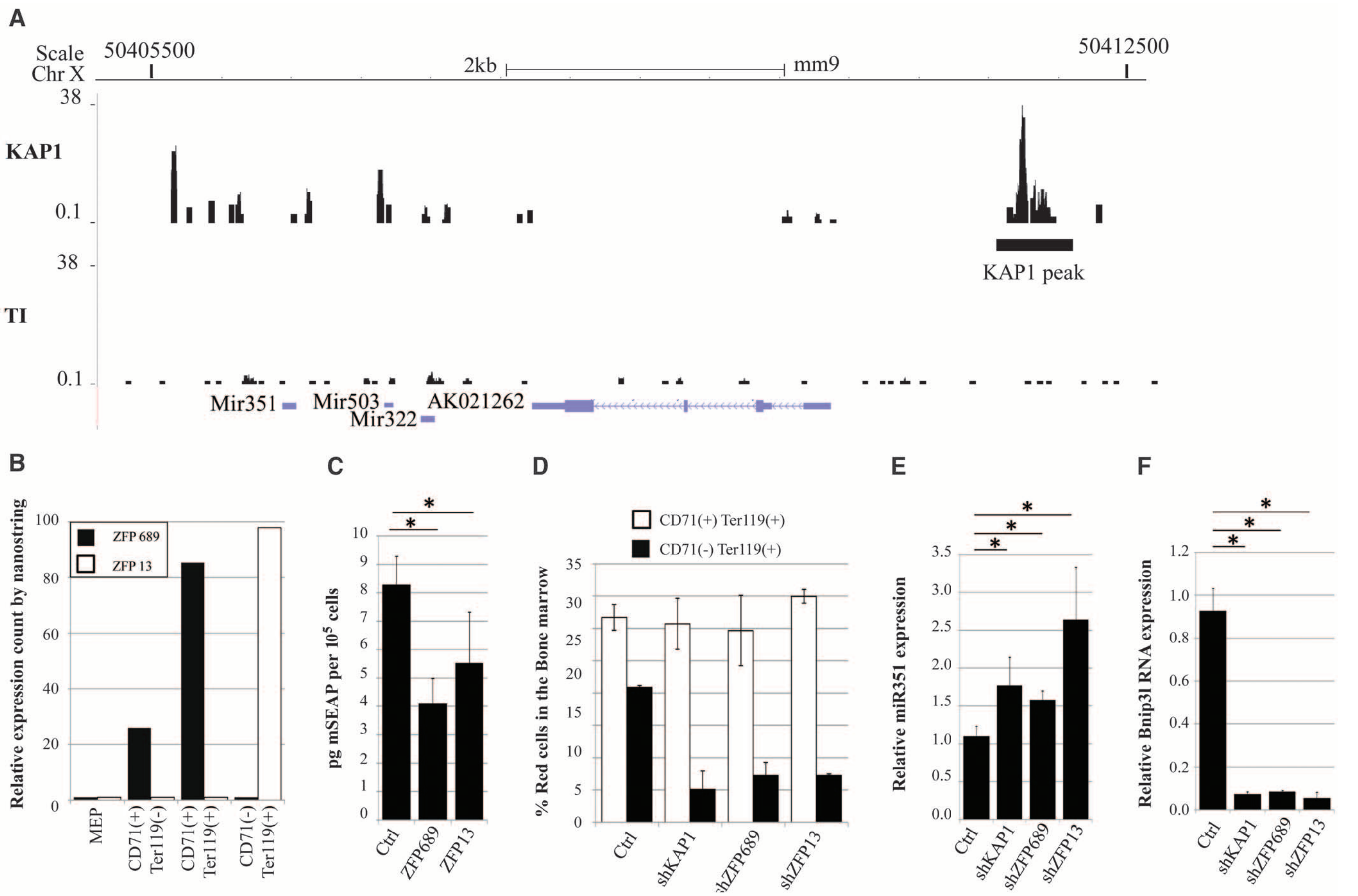

Fig. 3. Erythroblast-specific KRAB-ZFPs control the miR-351–Bnip3L-mitophagy axis. (**A**) Screen shots from the UCSC Genome Browser, with results of a KAP1 ChIP-seq analysis performed on CD71^{+} Ter119^{+} bone marrow cells. (**B**) *Zfp689* and *Zfp13* are induced during erythroid differentiation. (**C**) ZFP689 and ZFP13 repress a lentiviral vector carrying a miR-351–close KAP1-binding site in transduced MEL cells (Ctrl is a combination of ZFP-overexpressing cells transduced with a vector without the KAP1-binding site and LacZ-overexpressing cells transduced with a vector carrying the KAP1-binding site; $n = 3$, $*P < 0.05$). (**D**) CD45.2^{+} LSK cells were transduced with GFP-expressing, empty or scramble (Ctrl), *Kap1*-, *Zfp689*-, or *Zfp13*-directed shRNA lentiviral vectors, engrafted into irradiated CD45.1^{+} mice; erythroid differentiation was evaluated by FACS 8 weeks later. (**E** and **F**) The CD71^{+} Ter119^{+} CD45.2^{+} eGFP^{+} population was then sorted and analyzed by reverse transcription quantitative polymerase chain reaction (RT-qPCR) for miR-351 (E) and Bnip3L (F) expression ($n = 6$, $*P < 0.05$).

early erythroblasts and an almost complete absence of mature CD71$^-$ Ter119$^+$ cells in the bone marrow (Fig. 1A). Electron microscopy and MitoTracker staining revealed that *Kap1* KO erythroblasts contain more mitochondria than their wild-type counterparts (Fig. 1B), correlating with decreased expression of mitophagy transcripts such as *Nix/Bnip3L*, *Ulk1*, *Gabarapl2*, *Sh3glb1*, *Atg12*, *Becn1*, and *Bcl2l1* (Fig. 2A). Because the KRAB/KAP1 pathway is mostly known to induce transcriptional repression (*10*, *11*), it seemed likely that this effect was indirect. An examination of the microRNA (miRNA) expression profile of control and *Kap1* KO CD71$^+$ Ter119$^+$ cells revealed that among 455 miRNAs tested, 5 were down-regulated and 11 up-regulated by more than a factor of 2 in KO cells (data are presented in the Gene Expression Omnibus data set GSE44061).

A recently described in silico approach (*25*, *26*) suggested that six of these up-regulated miRNAs had mitophagy-associated deregulated transcripts as their targets, notably miR-351, predicted to act on *Bnip3L* (Fig. 2A). Consistent with this hypothesis, levels of miR-351 abruptly dropped in CD71$^+$ Ter119$^+$ cells relative to their CD71$^+$ Ter119$^-$ precursors, mirroring *Bnip3L* induction (Fig. 2B). Furthermore, transduction of mouse erythroleukemia (MEL) cells with a green fluorescent protein (GFP)–expressing lentiviral vector harboring, 3′ of GFP, the *Bnip3L* 3′ untranslated region (3′UTR) sequence predicted to be targeted by miR-351 resulted in miR-351–dependent down-regulation of the reporter (Fig. 2C). Finally, similar to their KAP1-depleted counterparts, miR-351–overexpressing MEL cells were blocked in differentiation and accumulated mitochondria, and this phenotype was reversed by expression of a *Bnip3L* transcript devoid of this 3′UTR sequence (fig. S2).

Both miR-503 and miR-322, which are located next to miR-351 on chromosome X, were also up-regulated (by factors of 2.46 and 2.17, respectively) in Kap1 KO erythroblasts. Consistent with a role for KRAB/KAP1 in regulating this miRNA gene cluster, chromatin immunoprecipitation coupled to DNA sequencing (ChIP-seq) detected a strong KAP1 peak less than 4 kb away (Fig. 3A). Because KAP1 is not a DNA binding protein, we postulated that it might be tethered to this and other relevant loci by stage-specific KRAB-ZFPs. Nine KRAB-ZFP genes were identified, which had human orthologs and were expressed exclusively in CD71$^+$ Ter119$^-$ and/or CD71$^+$ Ter119$^+$ erythroblasts but not in other hematopoietic cells. Six of these genes could be efficiently knocked down in MEL cells by lentivector-mediated RNA interference, and two of them, *Zfp689* and *Zfp13*, emerged as potential Bnip3L regulators (fig. S3). Interestingly, *Zfp689* is expressed in CD71$^+$ Ter119$^+$ erythroblasts, whereas *Zfp13* is expressed only in their CD71$^-$ Ter119$^+$ counterparts (Fig. 3B). Both could repress reporter expression in MEL cells transduced with a lentiviral vector harboring the miR-351–close KAP1-binding site upstream of a human phosphoglycerate kinase promoter mSEAP (murine secreted alkaline phosphatase) cassette (Fig. 3C). We then validated these two candidates in vivo by transplanting CD45.2 hematopoietic stem cells [lineage$^-$, Sca1$^+$, and cKit$^+$ (LSK)] transduced with lentiviral vectors producing GFP and short hairpin RNAs (shRNAs) against *Zfp689*, *Zfp13*, or *Kap1* (control) into irradiated CD45.1 mice, allowing the dual discrimination of donor versus recipient and transduced versus untransduced cells. Analyses of the red cell compartment in bone marrow harvested 8 weeks after the graft revealed that knockdown of either *Zfp689* or *Zfp13* led to a decrease in CD71$^-$ Ter119$^+$ cells as pronounced as that observed with the *Kap1* knockdown (Fig. 3D). Furthermore, RNA analyses of sorted transduced CD71$^+$ Ter119$^+$ cells demonstrated that ZFP689-, ZFP13-, and KAP1-depleted cells all exhibited an up-regulation of miR-351 (Fig. 3E) and a marked down-regulation of Bnip3L (Fig. 3F).

In a last series of experiments, we asked whether this erythropoiesis-regulating system has an equivalent in humans. We first found that *Kap1* knockdown impaired the differentiation of human erythroleukemia (HEL) cells and increased their mitochondrial content (Fig. 4, A to C), blocking several mitophagy effectors including *Nix/Bnip3L* (Fig. 4D). We further verified that KAP1-depleted HEL cells had increased levels of hsa-miR-125a-5p (Fig. 4D), which has the same miRNA seed as murine miR-351, and that overexpression of this miRNA triggered a down-regulation of Nix and a rise in the mitochondrial content of these cells (Fig. 4E). Finally, when we knocked down *Kap1* in human cord blood CD34$^+$ cells, it resulted in a decrease of their ability to undergo cytokine-induced ex vivo erythroid differentiation, which correlated with reduced Nix expression and elevated mitochondrial content (Fig. 4F)—a phenotype that could be reproduced by hsa-miR-125a overexpression (Fig. 4G).

These results indicate the presence of a multilayered transcription regulatory system in which protein- and RNA-based repressors are superimposed in combinatorial fashion to govern the timely triggering of a necessary step of erythropoiesis. miR-351 and several other miRNAs with predicted targets in the mitophagy pathway were up-regulated in *Kap1*-deleted murine erythroblasts (Fig. 2). This apparent redundancy—or, rather, addition of parallel effects aimed at the same physiological process—is commonly observed with RNA interference (*27*). Our discovery that it can be further modulated by KRAB-ZFP–mediated repression, and that the latter can itself be multifactorial, adds a remarkable level of modularity to this type of regulation. In human erythroblasts, although KAP1 represses the Nix-targeting hsa-miR-125a-5p, down-regulation of several other miRNAs (including hsa-miR-24, -221, -222, and -223) was previously found to be important for erythroid differentiation, which conversely requires the up-regulation of the hsa-miR-144/451 cluster (*2*, *3*). Whether stage-specific KRAB-ZFPs are involved in controlling some of these other miRNAs remains to be determined. Even though KAP1 likely influences erythropoiesis by more than just allowing mitophagy, it is interesting to note that *Znf205* and *Znf689*, the respective

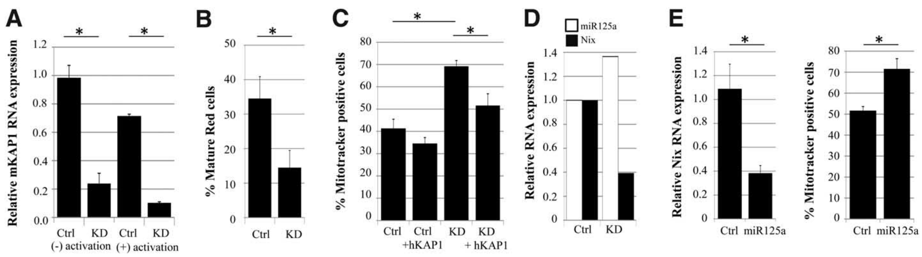

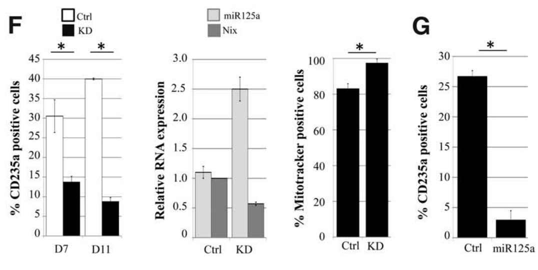

Fig. 4. KAP1-regulated RNA interference controls human red cell mitophagy. (**A** to **C**) HEL cells transduced with scramble or *Kap1*-specific shRNA-expressing lentiviral vectors and induced or not induced to differentiate were evaluated for *Kap1* mRNA expression (A) and by benzidine (B) ($n = 3$, counting 100 cells for each condition) or MitoTracker (C) ($n = 3$) staining ($^*P < 0.05$). (**D**) hsa-miR-125a-5p (miR125a) and Nix expression measured respectively by NanoString nCounter direct RNA quantification and RNA sequencing in HEL cells transduced with empty or *Kap1* knockdown vectors. (**E**) Nix expression in Ctrl (setting normalized value at 1) or hsa-miR-125a-5p–overexpressing HEL cells, measuring their mitochondrial content by MitoTracker staining ($n = 4$, $^*P < 0.05$). (**F**) Decreased erythroid differentiation of *Kap1* knockdown human cord blood CD34$^+$ cells, assessed by CD235a surface expression at 7 and 11 days (D7, D11). At D7, sorted CD235a$^+$ eGFP$^+$ cells were analyzed by RT-qPCR for Nix and hsa-miR-125a expression, and for mitochondrial content by MitoTracker staining ($n = 3$, $^*P < 0.05$). (**G**) Percentage of CD235a-expressing cells 7 days after inducing the differentiation of CD34$^+$ cells transduced with empty or unrelated miRNA–expressing (Ctrl) or hsa-miR-125a-5p–overexpressing lentiviral vectors ($n = 3$, $^*P < 0.05$).

human orthologs of murine *Zfp13* and *Zfp689*, are expressed in HEL cells and induced upon erythroid differentiation of $CD34^+$ cells (fig. S4). Therefore, polymorphism or mutations in any genetic component of the pathway unveiled here—whether *Znf205*, *Znf689*, the genomic binding sites of their products, hsa-miR-125a-5p and other KAP1-regulated miRNA genes, or the sequences targeted by these RNA regulators—could underlie red cell–related pathologies such as anemia, polycythemia, or erythroleukemia.

References and Notes

1. J. Xu *et al.*, *Dev. Cell* **23**, 796 (2012).
2. S. M. Hattangadi, P. Wong, L. Zhang, J. Flygare, H. F. Lodish, *Blood* **118**, 6258 (2011).
3. C. H. Lawrie, *Br. J. Haematol.* **150**, 144 (2010).
4. E. J. Bellefroid, D. A. Poncelet, P. J. Lecocq, O. Revelant, J. A. Martial, *Proc. Natl. Acad. Sci. U.S.A.* **88**, 3608 (1991).
5. J. M. Vaquerizas, S. K. Kummerfeld, S. A. Teichmann, N. M. Luscombe, *Nat. Rev. Genet.* **10**, 252 (2009).
6. J. C. Venter *et al.*, *Science* **291**, 1304 (2001).
7. A. T. Chinwalla *et al.*, *Nature* **420**, 520 (2002).
8. A. L. Nielsen *et al.*, *EMBO J.* **18**, 6385 (1999).
9. S. Quenneville *et al.*, *Cell Rep.* **2**, 766 (2012).
10. D. C. Schultz, K. Ayyanathan, D. Negorev, G. G. Maul, F. J. Rauscher 3rd, *Genes Dev.* **16**, 919 (2002).
11. D. C. Schultz, J. R. Friedman, F. J. Rauscher 3rd, *Genes Dev.* **15**, 428 (2001).
12. H. M. Rowe *et al.*, *Nature* **463**, 237 (2010).
13. H. M. Rowe *et al.*, *Genome Res.* **23**, 452 (2012).
14. D. Wolf, S. P. Goff, *Cell* **131**, 46 (2007).
15. K. Bojkowska *et al.*, *Hepatology* **56**, 1279 (2012).
16. S. Chikuma, N. Suita, I. M. Okazaki, S. Shibayama, T. Honjo, *Nat. Immunol.* **13**, 596 (2012).
17. J. Jakobsson *et al.*, *Neuron* **60**, 818 (2008).
18. X. Li *et al.*, *Dev. Cell* **15**, 547 (2008).
19. D. J. Mackay *et al.*, *Nat. Genet.* **40**, 949 (2008).
20. F. R. Santoni de Sio *et al.*, *FASEB J.* 10.1096/fj.12-206177 (2012).
21. F. R. Santoni de Sio *et al.*, *Blood* **119**, 4675 (2012).
22. J. H. Shin *et al.*, *Cell* **144**, 689 (2011).
23. L. Zheng *et al.*, *Mol. Cell* **6**, 757 (2000).
24. Y. Ziv *et al.*, *Nat. Cell Biol.* **8**, 870 (2006).
25. R. M. Marín, J. Vaníček, *Nucleic Acids Res.* **39**, 19 (2011).
26. R. M. Marín, J. Vaníček, *PLoS ONE* **7**, e32208 (2012).
27. M. S. Ebert, P. A. Sharp, *Cell* **149**, 515 (2012).

Acknowledgments: We thank the staff of our core facilities for technical expertise, and P. Turelli, B. Yazdanpanah, and F. Marzetta (EPFL), P. Malik (Cincinnati Children's Hospital), and G. Ferrari (San Raffaele Telethon Institute for Gene Therapy, Milano) for the kind gift of reagents. Supported by grants from the Swiss National Science Foundation and the European Research Council (D.T.). The cDNA and miRNA microarray and ChIP-seq data are deposited in the Gene Expression Omnibus (www.ncbi.nlm.nih.gov/geo) under accession number GSE44061. D.T. and I.B. are inventors on a patent application submitted by EPFL for the control of mitophagy.

Supplementary Materials

www.sciencemag.org/cgi/content/full/science.1232398/DC1
Materials and Methods
Figs. S1 to S4
Table S1
References (*28–38*)

5 November 2012; accepted 26 February 2013
Published online 14 March 2013;
10.1126/science.1232398

The Helicase-Like Domains of Type III Restriction Enzymes Trigger Long-Range Diffusion Along DNA

Friedrich W. Schwarz,[1]* Júlia Tóth,[2]* Kara van Aelst,[2] Guanshen Cui,[2] Sylvia Clausing,[1] Mark D. Szczelkun,[2]† Ralf Seidel[1,3]†

Helicases are ubiquitous adenosine triphosphatases (ATPases) with widespread roles in genome metabolism. Here, we report a previously undescribed functionality for ATPases with helicase-like domains; namely, that ATP hydrolysis can trigger ATP-independent long-range protein diffusion on DNA in one dimension (1D). Specifically, using single-molecule fluorescence microscopy we show that the Type III restriction enzyme EcoP15I uses its ATPase to switch into a distinct structural state that diffuses on DNA over long distances and long times. The switching occurs only upon binding to the target site and requires hydrolysis of ~30 ATPs. We define the mechanism for these enzymes and show how ATPase activity is involved in DNA target site verification and 1D signaling, roles that are common in DNA metabolism: for example, in nucleotide excision and mismatch repair.

Helicases were defined classically as adenosine triphosphatases (ATPases) that use directional translocation to unwind duplex nucleic acids. More recently, however, many "pseudo-helicases" have been described that possess amino acid motifs characteristic of helicases yet fulfill their cellular functions without obligate DNA unwinding (*1*) and instead are often translocases that move directionally on single- (*2*) or double-stranded (*3*, *4*) nucleic acids. Pseudo-helicases include the ATP-dependent bacterial Type I and III restriction enzymes (REs), which use ATP hydrolysis to communicate between two distant restriction sites on the same DNA (*5*, *6*). Only if both sites are unmethylated is the DNA considered "foreign" and destroyed by the endonuclease. Type III REs form a heterooligomeric complex of two subunits: Mod (for target site methylation) and Res (for ATPase and endonuclease activities). Because they only hemimethylate their asymmetric recognition sequences, these enzymes must signal the relative site orientation during communication (*7*): Cleavage occurs only if the sites are in an inverted-repeat orientation, arranged either "head-to-head" (HtH) (*7*) or "tail-to-tail" (TtT) (*8*). Type III REs hydrolyze only a few tens of ATPs per double-stranded DNA (dsDNA) break (*9*, *10*), suggesting either passive three-dimensional (3D) looping between sites with limited translocation (*11*) or diffusion in 1D following an ATP-dependent switch (fig. S1A) (*8*, *10*).

To distinguish between the different communication models, we developed a real-time single-molecule assay using magnetic tweezers combined with total internal reflection fluorescence (TIRF) microscopy (*12*) that can localize fluorescently labeled enzymes on stretched 26–kilobase pair (kbp) DNA molecules containing two centrally located HtH EcoP15I sites with 6-kbp intersite distance (Fig. 1A). EcoP15I was labeled with quantum dots on the C terminus of the Res subunit (QR-EcoP15I), without compromising the biochemical activity (fig. S2). Whereas DNA binding by lone quantum dots was not detected, addition of QR-EcoP15I and ATP resulted in enzyme attachment at one (Fig. 1B and movie S1) or two (fig. S3) specific recognition sites. Enzymes always arrived instantaneously at the sites, with no evidence for long-lived, nonspecific binding en route ($N = 61$). After a delay of, on average, 17 ± 2 s (fig. S4), bound enzymes started to move rapidly in both directions along the DNA (Fig. 1B), consistent with random walk simulations using measured parameters (*13*) (fig. S5). All bound enzyme complexes ($N = 91$) could be assigned to one of the two target sites (fig. S6A), and 90% exhibited fast bidirectional movement. The mean-square displacement determined from single-particle tracking time trajectories (*14*) was found to increase linearly with time, confirming a 1D diffusion with a diffusion constant $D = 0.92 \pm 0.06\ \mu m^2\ s^{-1}$ (Fig. 1C). This is one of the highest values reported, suggesting that EcoP15I is optimized for rapid, long-distance DNA scanning (supplementary text). Rebinding to the original site or a second distant specific site was often observed, after which additional sliding events could restart with a similar initiation rate (fig. S4) until final dissociation occurred. Rebinding occurred preferentially at sites with the same orientation as the start site (Fig. 1D and fig. S4). The average lifetime of a diffusion event was 9 ± 1 s, whereas the average total DNA interaction time involving multiple sliding and rebinding events was 180 ± 10 s (fig. S4). Thus, an enzyme can explore thousands of base pairs up- and downstream of the original site before dissociation. On a substrate with a sufficient density of EcoP15I

[1]DNA motors group, Biotechnology Center, Technische Universität Dresden, 01062 Dresden, Germany. [2]DNA-Protein Interactions Unit, School of Biochemistry, Medical Sciences Building, University of Bristol, Bristol BS8 1TD, UK. [3]Institute of Molecular Cell Biology, University of Münster, 48149 Münster, Germany.

*These authors contributed equally to this work.
†Corresponding author. E-mail: mark.szczelkun@bristol.ac.uk (M.D.S.); ralf.seidel@uni-muenster.de (R.S.)

A KRAB/KAP1-miRNA Cascade Regulates Erythropoiesis Through Stage-Specific Control of Mitophagy
Isabelle Barde, Benjamin Rauwel, Ray Marcel Marin-Florez, Andrea Corsinotti, Elisa Laurenti, Sonia Verp, Sandra Offner, Julien Marquis, Adamandia Kapopoulou, Jiri Vanicek and Didier Trono
(March 14, 2013)
Science **340** (6130), 350-353. [doi: 10.1126/science.1232398]
originally published online March 14, 2013

Editor's Summary

Red in Cell and Marrow

About one hundred billion new red cells are released every day from the adult human bone marrow––the result of a complex differentiation pathway. **Barde *et al.*** (p. 350, published online 14 March) show that an essential step in this process, the elimination of mitochondria from maturing erythroblasts through mitophagy, is controlled through the timely induction of specific members of the large family of KRAB-containing zinc finger proteins (KRAB-ZFPs), which, together with their cofactor KAP1, repress the expression of micro-RNAs targeting the transcripts of mitophagy effector genes. This multilayered and combinatorial regulation system provides a level of modularity that may be shared by other physiological processes.